Efficient modelling of channel maps with correlated shadow fading in mobile radio systems

Holger Claussen
Bell Laboratories, Lucent Technologies
The Quadrant, Stonehill Green
Swindon SN5 7DJ, United Kingdom
Email: claussen@lucent.com

Abstract— **For simulating mobility of both user terminals and base stations in wireless access systems, it is often advantageous to generate environment "maps" of the channel attenuations including path loss and shadow fading. However, the generation of a large number of spatially correlated shadow fading values, using for example the Cholesky decomposition of the corresponding correlation matrix, is computationally complex and requires a large amount of memory. In this paper an efficient low complexity alternative is proposed, where each new fading value is generated based only on the correlation with selected neighbouring values in the map. This results in a significant reduction of the computational complexity and memory requirements. It is shown that taking a small number of neighbouring values into account is sufficient to achieve relatively small correlation errors in the generated shadow fading maps.**

I. Introduction

In system level simulations which support mobility of both user terminals and base stations, it is often advantageous to generate a channel environment of the area of interest in the form of a 2 dimensional "map", including the effects of path loss and shadow fading as shown in Fig. 1. In contrast to [1], where the shadow fading correlations are derived based on the mobile velocity, the use of channel maps allows one to define a channel environment with specific channel attenuations at all potential mobile locations.

While calculating the path loss for each value in the map is relatively simple, the generation of shadow fading attenuations, representing the variations of the channel loss caused by obstacles in the path between the mobile and the base station, is more difficult due to their spatial correlation properties. The conventional way of generating correlated shadow fading values is the pre-multiplication of independent random variables with a suitable decomposition (e.g. Cholesky factor) of the corresponding correlation matrix, as described in more detail in Section III-A. A major problem of this approach is the vast number of correlated shadow fading values required. This results in large correlation matrices even for a limited map size.

For shadow fading maps with $n \times m$ elements, generated using the Cholesky decomposition, the memory requirements for the correlation matrix are $(nm)^2$ fading values. The computational complexity of the corresponding Cholesky decomposition involves $(nm)^3/6$ multiplications and subtractions, and also nm square roots [2].

Example:

A small shadow fading map with 200×200 elements already contains 40000 elements. This results in a correlation matrix of the size 40000×40000. With 4 bytes per value, this would require 6.4 GB of memory. In addition, the Cholesky decomposition of such a large matrix involves a significant computational complexity (2.13×10^{13} operations).

As a result, the conventional method is not suited for the generation of shadow fading maps in system level simulators due to its prohibitive computational complexity and memory requirements. This is particularly the case when considering base station mobility, which requires the generation of new channel maps for each new base station position. Alternative approaches based on the sum of sinusoid method were presented in [3].

In this paper, a novel low complexity method for the generation of correlated shadow fading maps is proposed and analysed. Section II provides the necessary background on channel modelling based on path loss and shadow fading. In Section III, the generation of correlated shadow fading maps is discussed and a low complexity method is proposed, where each new fading value is generated based only on the

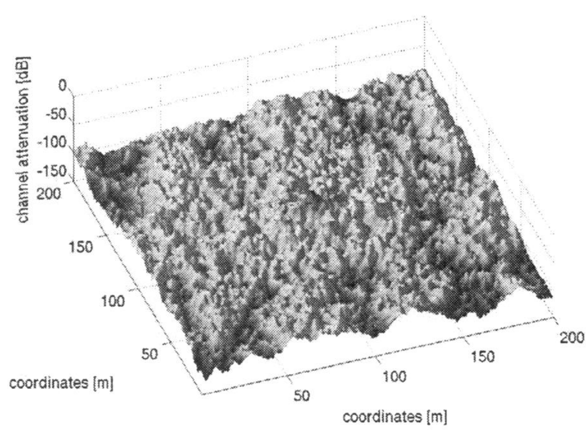

Fig. 1. Example of a generated channel attenuation map with 200×200 elements including path loss and shadow fading for a base station at the coordinates (100m,100m), and spatial correlations of $r(x) = e^{-x/20}$

978-3-8007-2909-8/05/$20.00 ©2005 IEEE

correlation with selected neighbouring values in the map. The accuracy and the computational complexity of the proposed method is analysed in Section IV. Finally, conclusions are drawn in Section V.

II. BACKGROUND

In mobile radio systems the propagation medium between two nodes is called the channel, and results in an attenuation of the transmitted signal. It can be characterised as a combination of attenuations resulting from path loss, shadow fading and multipath fading. Multipath fading has been extensively studied in the literature [4]. In system-level simulations, the influence of multipath fading is usually accounted for in the frame-error rate results of link-level simulations and is therefore not investigated here. This paper is focused on the other contributions, namely path loss and shadow fading. When all quantities are expressed in decibels (dB), the received signal power can be written as

$$P_{\mathrm{rx}}|_{\mathrm{dB}} = P_{\mathrm{tx}}|_{\mathrm{dB}} + G_{\mathrm{BS}}|_{\mathrm{dB}} + G_{\mathrm{UE}}|_{\mathrm{dB}} - L_{\mathrm{p}}|_{\mathrm{dB}} - L_{\mathrm{s}}|_{\mathrm{dB}}, \quad (1)$$

where P_{tx} is the transmitted power, L_{p} is the path loss and L_{s} is the attenuation resulting from shadow fading. G_{BS} denotes the base station (BS) antenna gain and G_{UE} is the user equipment (UE) antenna gain (including cable losses). Typical values for G_{BS} and G_{UE} in picocell scenarios are given in [5] as 11 dB and 0 dB respectively.

A. Path loss model

For the path loss calculation, it is assumed that the transmitted power is radiated from an isotropic radiator. Then, the path loss can be written as a combination of losses $L_{\mathrm{r}}(d)$ resulting from the propagation and reception of the signal at a distance d, and $L_{\mathrm{w}}(d)$ due to propagation through walls:

$$L_{\mathrm{p}}|_{\mathrm{dB}} = L_{\mathrm{r}}(d)|_{\mathrm{dB}} + L_{\mathrm{w}}(d)|_{\mathrm{dB}}, \quad (2)$$

where all entities are given in dB. The propagation loss [6] may be written as

$$L_{\mathrm{r}}(d)|_{\mathrm{dB}} = -20\log_{10}\left(\frac{\lambda}{4\pi}\right) + 20\log_{10}(d), \quad (3)$$

where $\lambda = c/f_c$ denotes the wavelength of the carrier frequency, c denotes the speed of light ($\simeq 3 \times 10^8$ m/s) and f_c is the carrier frequency. The losses due to walls may be modelled implicitly as given in COST 231 dependent on the distance d as:

$$L_{\mathrm{w}}(d)|_{\mathrm{dB}} = 10\log_{10}(d). \quad (4)$$

An alternative explicit wall model is presented in [5]. For a UMTS scenario with a carrier frequency of 2 GHz, this results in a path loss of $L_{\mathrm{p,UMTS}} = 38.5 + 30\log_{10}(d)$ dB.

B. Shadow fading model

Shadow fading represents the variations in the channel loss caused by obstacles in the propagation path between the mobile and the base station. It is usually modelled as a log-normal distributed random variable with zero-mean L_{s} [7].

A typical value for the shadow fading standard deviation for an indoor environment is $\sigma_{\mathrm{s}} = 12$ dB for implicitly modelled walls. In [5], a much lower value of 6 dB is used, which is suitable for an explicit wall model.

C. Spatial correlation of shadow fading

To simulate mobility of user terminals or base stations, the spatial correlations of the shadow fading values need to be taken into account. In [1], a simple exponential correlation model was proposed. Using a spatial variable instead of time for the shadowing process [7], the normalised correlation function can be written as

$$r(x) = e^{-\alpha x}, \qquad x \geq 0, \quad (5)$$

where $e^{-\alpha}$ is the correlation coefficient between two points spaced by a distance $x = 1$. In [8], a value of $\alpha = 1/20$ is suggested for an environment intermediate between suburban and urban microcellular.

III. GENERATION OF CORRELATED SHADOW FADING MAPS

The generation of a large number of correlated shadow fading values involves significant computational complexity and memory requirements, as shown in Section I. The conventional approach using the Cholesky decomposition of the corresponding correlation matrix is described below. In addition, a simplified approach is proposed which allows the generation of large correlated shadow fading "maps" at a low computational complexity.

A. Conventional approach

Specified correlations between several randomly generated uncorrelated shadow fading values in a vector $\mathbf{a}$ with $\mathrm{E}\{\mathbf{a}\mathbf{a}^{\mathrm{T}}\} = \mathbf{I}$ can be achieved by a multiplication with the Cholesky factor $\mathbf{L}$ of the correlation matrix $\mathbf{R}$:

$$\mathbf{s} = \mathbf{L}\mathbf{a}. \quad (6)$$

Given that $\mathrm{E}\{\mathbf{a}\mathbf{a}^{\mathrm{T}}\} = \mathbf{I}$ it is easy to see that $\mathrm{E}\{\mathbf{s}\mathbf{s}^{\mathrm{T}}\} = \mathbf{L}\mathbf{L}^{\mathrm{T}} = \mathbf{R}$. However, to generate a large amount of correlated shadow fading values, the complexity of the generation of the correlation matrix $\mathbf{R}$, and its the Cholesky decomposition, becomes prohibitive.

B. Low complexity approach

The computational complexity can be reduced significantly by deriving the fading values based only on the correlation with respect to the neighbouring values in the map. For the simple example of three fading values shown in Fig. 2, each of the shadow fading values s_1, s_2, and s_3 can be calculated using (5) and (6) with the correlation matrix

$$\mathbf{R} = \begin{bmatrix} 1 & r(x) \\ r(x) & 1 \end{bmatrix} \text{ and } \mathbf{L} = \begin{bmatrix} 1 & 0 \\ r(x) & \sqrt{1 - r^2(x)} \end{bmatrix}. \quad (7)$$

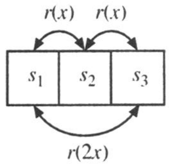

Fig. 2. Simplified generation of correlated fading values.

The resulting fading values s_2 and s_3 may be written as

$$s_1 = a_1 \tag{8}$$

$$s_2 = r(x)s_1 + \sqrt{1-r^2(x)}\ a_2 \tag{9}$$

$$\begin{aligned} s_3 &= r(x)s_2 + \sqrt{1-r^2(x)}\ a_3 \\ &= r^2(x)s_1 + r(x)\sqrt{1-r^2(x)}\ a_2 \\ &\quad + \sqrt{1-r^2(x)}\ a_3. \end{aligned} \tag{10}$$

The components a_1, a_2, and a_3 are generated in dB as normally distributed random variables with standard deviation $\sigma_{\rm s}$ as discussed in Section II-B. This results in the following correlations: $\mathrm{E}\{s_1 s_2\} = \sigma_{\rm s}^2 r(x)$, $\mathrm{E}\{s_2 s_3\} = \sigma_{\rm s}^2 r(x)$ and $\mathrm{E}\{s_1 s_3\} = \sigma_{\rm s}^2 r^2(x)$. Note that the correlation $\mathrm{E}\{s_1 s_3\}$ should be equal to $\sigma_{\rm s}^2 r(2x)$ due to the distance of $2x$ between s_1 and s_3. However, the exponential model of (5) for the shadow fading correlation has the following useful property:

$$r(kx) = e^{-\alpha k x} = \left(e^{-\alpha x}\right)^k = r^k(x), \tag{11}$$

which, for $k = 2$, is equal to the correlation result of $\mathrm{E}\{s_1 s_3\}$ obtained using the proposed simplified generation method. Therefore, although the generation of fading value s_3 is based only on the correlation with its nearest neighbour s_2, the method automatically results also in the correct correlation with s_1 of $\sigma_{\rm s}^2 r^2(x) = \sigma_{\rm s}^2 r(2x)$ when an exponential model in the form of (5) is used for the shadow fading correlation.

This concept may be extended to efficiently generate a two-dimensional "map" of spatially correlated shadow fading values by taking only the neighbouring values into account for the correlation operation. This procedure is illustrated in Fig. 3. A given set of correlated fading values $\tilde{\mathrm{s}} = (s_1, s_2, s_3, s_4)^{\rm T}$ with the correlation $\mathrm{E}\{\tilde{\mathrm{s}}\tilde{\mathrm{s}}^{\rm T}\} = \tilde{\mathbf{R}}$ shall be extended to $\mathrm{s} = (s_1, s_2, s_3, s_4, s_{\rm n})^{\rm T}$ with the correlation $\mathrm{E}\{\mathrm{s}\mathrm{s}^{\rm T}\} = \mathbf{R}$. The coefficients of $\tilde{\mathbf{R}}$ and $\mathbf{R}$ are calculated using (5), dependent on the corresponding spatial distances between the fading values shown in Fig. 3.

For this, the condition $\mathrm{s} = \mathbf{L}\mathrm{a}$ in (6) must be satisfied, where the elements $a_1 \ldots a_4$ of vector a, and the new fading value $s_{\rm n}$ are unknown:

$$\mathrm{s} = \mathbf{L}\mathrm{a} = \mathbf{L}\begin{bmatrix} \tilde{\mathbf{L}}^{-1}\tilde{\mathrm{s}} \\ a_{\rm n} \end{bmatrix} \tag{12}$$

where $a_{\rm n}$ is generated in dB as a normal distributed random variable as described in Section II-B. Therefore, the new correlated fading value can be written as

$$s_{\rm n} = \lambda_{\rm n}^{\rm T}\begin{bmatrix} \tilde{\mathbf{L}}^{-1}\tilde{\mathrm{s}} \\ a_{\rm n} \end{bmatrix} \tag{13}$$

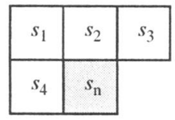

Fig. 3. Generation of a correlated fading value in a 2 dimensional space taking four neighbours into account.

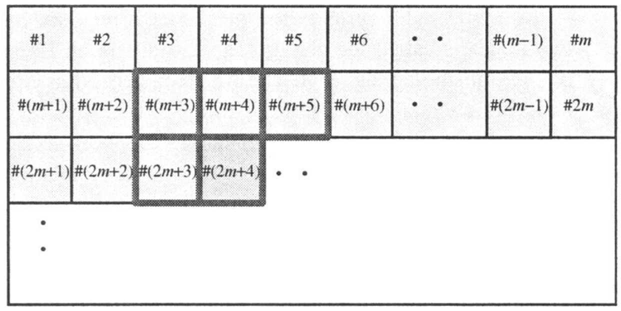

Fig. 4. Generation of a 2 dimensional correlated fading map taking four neighbours into account.

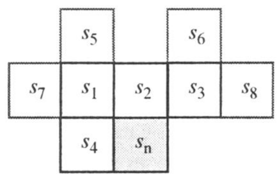

Fig. 5. Generation of a correlated fading value in a 2 dimensional space taking eight neighbours into account.

where $\lambda_{\rm n}^{\rm T}$ is the last row of $\mathbf{L}$. Using this scheme for each new fading value, a map of correlated shadow fading values can be generated very efficiently as shown in Fig. 4. For initialisation and at the edges of the map, only available values are taken into account for the generation of each new shadow fading value (e.g. for the generation of value #2, only #1 is taken into account; for the generation of value $\#2m$, the neighbours $\#(2m-1)$, $\#(m-1)$, and $\#m$ are taken into account).

Note that, although the fading values are generated in a way that the correlations with all nearest neighbouring values are correct, this simplification results in small correlation errors with values in directions that were not taken into account. These errors can be reduced by increasing the number of neighbouring values for the generation of each new value, as shown in Fig. 5 for 8 neighbours. Here, the neighbours were selected to maximise the directions of correct correlation with a minimum number of required values.

C. Correlations between multiple base stations

When base stations are located in a similar environment as mobiles, the correlations between the corresponding fading maps can be determined from (5) using the same value of α, and the maps can be correlated similar to single fading values using the coefficients of $\mathbf{L}$ in (6). Alternatively, a

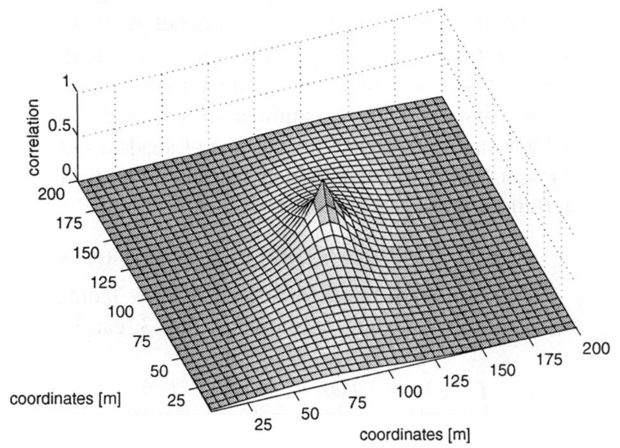

Fig. 6. Mean values of the generated spatial correlation with respect to a reference point at the coordinates $(100m \times 100m)$, taking four neighbours into account. It is shown that in this case the resulting correlations are slightly asymmetric, resulting in a clearly visible correlation error.

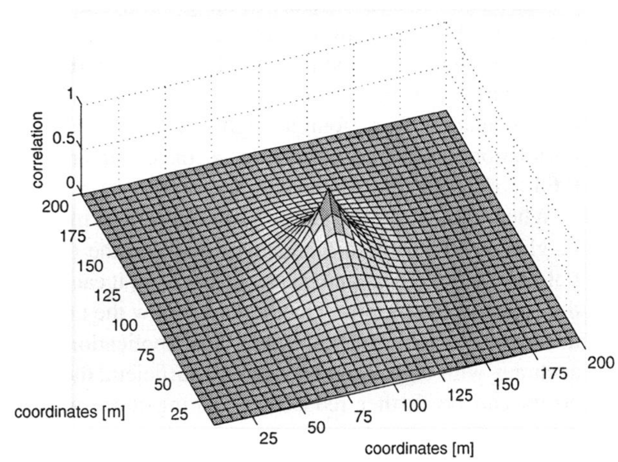

Fig. 8. Mean values of the generated spatial correlation with respect to a reference point at the coordinates $(100m \times 100m)$, taking eight neighbours into account. Here, the resulting correlations are more symmetric and the correlation error is reduced significantly compared to Fig. 6

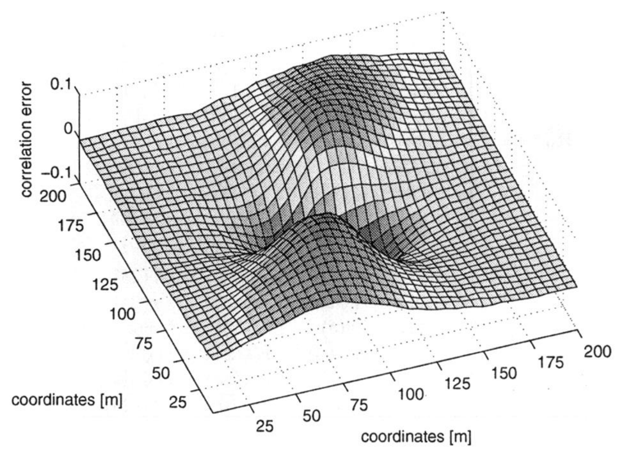

Fig. 7. Errors of the spatial correlations shown in Fig. 6 with respect to a reference point at the coordinates $(100m \times 100m)$, taking four neighbours into account.

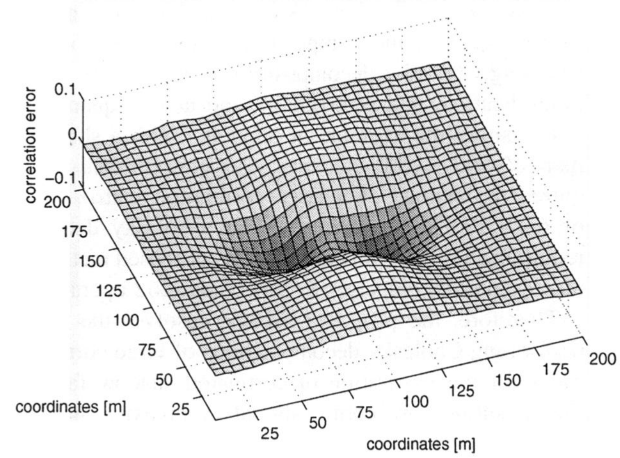

Fig. 9. Errors of the spatial correlations shown in Fig. 8 with respect to a reference point at the coordinates $(100m \times 100m)$, taking eight neighbours into account.

constant correlation between base stations may be assumed for simplicity [9], arguing that the shadow fading depends mainly on the environment close to the mobile, when base stations are located at higher points (e.g. on top of buildings).

IV. Results

In this section, the errors and the efficiency (i.e. computational complexity and memory requirements) of the proposed low complexity method for the generation of correlated shadow fading maps are investigated.

A. Error analysis of the proposed method

In order to evaluate the errors resulting from the proposed simplified method, correlations of the generated maps with respect to a reference point in the centre of each map are computed in 10^5 trials. Then the obtained correlation values are compared with the exact correlations calculated from (5). For this test, a small area of $200\mathrm{m} \times 200\mathrm{m}$ is considered with 40×40 generated fading values per map.

Fig. 6 illustrates the resulting mean correlation values of the generated maps based on four neighbouring values as shown in Fig. 3, with respect to a reference point at the coordinates $(100\mathrm{m}, 100\mathrm{m})$. The corresponding normalised mean correlation error is shown in Fig. 7. It is shown that using four neighbouring values results in a slightly asymmetric correlation with a mean squared error of 2.3×10^{-3} for the simulated scenario.

The mean correlation values of the generated maps based on eight neighbouring values is illustrated in Fig. 8 for the same scenario. The corresponding normalised mean correlation error is shown in Fig. 9. Increasing the number of neighbours for the calculation from four to eight, reduces the asymmetric correlation error and results in a mean squared error of 0.63×10^{-3} for the simulated scenario.

When comparing the errors of the proposed method (eight neighbours) with the discrepancies between the the exponential correlation model and measured data [1], it can be seen that the errors of the proposed method are below the uncertainty of the exponential correlation model. For applications where the accuracy with eight neighbours is not sufficient, the correlation errors can be further reduced by taking more neighbouring values into account for the generation.

B. Computational complexity and memory requirements

Taking only the neighbouring values into account for the calculation of the correlated shadow fading values reduces both memory requirements and computational complexity significantly. For shadow fading maps with $n \times m$ elements, the size of the correlation matrix is reduced from $(nm)^2$ values to only $(w+1)^2$ when taking w neighbours into account. In consequence, the computational complexity of the corresponding Cholesky decomposition is reduced to $(w+1)^3/6$ multiplications and subtractions, and $w+1$ square roots.

Revisiting the example in Section I with a shadow fading map of 200×200 elements, the conventional method required the storage of a large correlation matrix of the size of 6.4 GB and the corresponding Cholesky decomposition required 2.13×10^{13} operations. The proposed method reduces these values significantly to 324 B and 252 operations.

Therefore, the proposed method resolves the problem of performing Cholesky decompositions of large correlation matrices for the generation of correlated shadow fading maps. The resulting low computational complexity, which scales linearly with the number of required shadow fading values, enables an efficient use of shadow fading maps in system level simulators. This is especially important in systems with base station mobility, where new channel maps must be generated (and correlated with the previous ones) for every new base station position.

V. Conclusions

In this paper, the generation of channel attenuation maps, incorporating path loss and spatially correlated shadow fading, was investigated to support mobility for user terminals and base stations in system level simulations. It was shown that the generation of large numbers of correlated shadow fading values using the Cholesky decomposition of the corresponding correlation matrix results in prohibitive computational complexity and memory requirements. An efficient method for generating correlated shadow fading maps was proposed, where each new fading value is generated based only on the correlation with selected neighbouring values in the map. It was demonstrated that a low number of neighbouring values are sufficient to reduce the correlation errors resulting from the proposed method, to a level which is below the uncertainty of the exponential correlation model when compared to measured data. This results in a low computational complexity, which scales linearly with the number of required shadow fading values, and enables an efficient use of shadow fading maps in system level simulators which support mobility for both user terminals and base stations.

Appendix: Correlation Matrices

The correlation matrices for the shadow fading generation using four neighbours, as shown in Fig. 3, can be written as

$$\mathbf{R}_5 = \begin{pmatrix} 1 & r(\delta) & r(2\delta) & r(\delta) & r(\sqrt{2}\delta) \\ r(\delta) & 1 & r(\delta) & r(\sqrt{2}\delta) & r(\delta) \\ r(2\delta) & r(\delta) & 1 & r(\sqrt{5}\delta) & r(\sqrt{2}\delta) \\ r(\delta) & r(\sqrt{2}\delta) & r(\sqrt{5}\delta) & 1 & r(\delta) \\ r(\sqrt{2}\delta) & r(\delta) & r(\sqrt{2}\delta) & r(\delta) & 1 \end{pmatrix}, \quad (14)$$

where δ denotes the distance in metres between two adjacent shadow fading values in the map. The correlation matrices for the fading generation using eight neighbours, as shown in Fig. 5 can be written as

$$\mathbf{R}_9 = \left(\begin{array}{cccccc} 1 & r(\delta) & r(2\delta) & r(\delta) & r(\delta) & \dots \\ r(\delta) & 1 & r(\delta) & r(\sqrt{2}\delta) & r(\sqrt{2}\delta) & \dots \\ r(2\delta) & r(\delta) & 1 & r(\sqrt{5}\delta) & r(\sqrt{5}\delta) & \dots \\ r(\delta) & r(\sqrt{2}\delta) & r(\sqrt{5}\delta) & 1 & r(2\delta) & \dots \\ r(\delta) & r(\sqrt{2}\delta) & r(\sqrt{5}\delta) & r(2\delta) & 1 & \dots \\ r(\sqrt{5}\delta) & r(\sqrt{2}\delta) & r(\delta) & r(\sqrt{8}\delta) & r(2\delta) & \dots \\ r(\delta) & r(2\delta) & r(3\delta) & r(\sqrt{2}\delta) & r(\sqrt{2}\delta) & \dots \\ r(\delta 3) & r(2\delta) & r(\delta) & r(\sqrt{10}\delta) & r(\sqrt{10}\delta) & \dots \\ r(\sqrt{2}\delta) & r(\delta) & r(\sqrt{2}\delta) & r(\delta) & r(\sqrt{5}\delta) & \dots \end{array}\right.$$

$$\left.\begin{array}{ccccc} \dots & r(\sqrt{5}\delta) & r(\delta) & r(3\delta) & r(\sqrt{2}\delta) \\ \dots & r(\sqrt{2}\delta) & r(2\delta) & r(2\delta) & r(\delta) \\ \dots & r(\delta) & r(3\delta) & r(\delta) & r(\sqrt{2}\delta) \\ \dots & r(\sqrt{8}\delta) & r(\sqrt{2}\delta) & r(\sqrt{10}\delta) & r\delta \\ \dots & r(2\delta) & r(\sqrt{2}\delta) & r(\sqrt{10}\delta) & r(\sqrt{5}\delta) \\ \dots & 1 & r(\sqrt{10}\delta) & r(\sqrt{2}\delta) & r(\sqrt{5}\delta) \\ \dots & r(\sqrt{10}\delta) & 1 & r(4\delta) & r(\sqrt{5}\delta) \\ \dots & r(\sqrt{2}\delta) & r(4\delta) & 1 & r(\sqrt{5}\delta) \\ \dots & r(\sqrt{5}\delta) & r(\sqrt{5}\delta) & r(\sqrt{5}\delta) & 1 \end{array}\right). \quad (15)$$

References

[1] M. Gudmundson, 'Correlation model for shadow fading in mobile radio systems," *Electron. Lett.*, vol. 27, no. 2, pp. 2145-2146, Nov. 1991.

[2] W. H. Press, S. A. Teukolsky, W. T. Vetterling, B. P. Flannery, *Numerical recipes in C++*. Cambridge University Press, 2002.

[3] X. Cai, G. B. Giannakis, 'A two-dimensional channel simulation model for shadowing processes," *IEEE Trans. Vehicular Technology*, vol. 52, no. 6, pp. 1558-1567, Nov. 2003.

[4] W. C. Jakes, *Microwave mobile communication*. Wiley, 1974.

[5] 3GPP TSG RAN, TR 25.951 v6.2.0, 'FDD base station (BS) classification (release 6)," Oct. 2003.

[6] B. Sklar, *Digital communications - Fundamentals and applications*. Prentice Hall PTR, 2001.

[7] D. Giancristofaro, 'Correlation model for shadow fading in mobile radio channels," *Electron. Lett.*, vol. 32, no. 11, pp. 858-959, May 1996.

[8] R. Vijayan, J. M. Holtzman 'The dynamic behaviour of handoff algorithms," in *proc. ICUPC*, pp. 02.03/5-1, Sept. 1992

[9] 3GPP TSG RAN, TR 25.942 v6.4.0, 'Radio frequency (RF) system scenarios (release 6)," Apr. 2005.